A detailed comparison of the Dutch emission inventory with satellite-derived NO$_x$ emissions

Hannes Witt[1], Ronald J. van der A[2], Jieying Ding[2], Jeroen Kuenen[4], Margreet C. van Zanten[1,3]

[1] National Institute for Public Health and the Environment (RIVM), Bilthoven, The Netherlands
[2] Royal Netherlands Meteorological Institute (KNMI), De Bilt, The Netherlands
[3] Meteorology and Air Quality Section, Wageningen University, Wageningen, The Netherlands
[4] Department of Climate, Air and Sustainability, TNO, Utrecht, The Netherlands

Correspondence to: H. Witt (Hannes.witt@rivm.nl)

Abstract. Nitrogen oxides are one of the most important air pollutants with a large impact on human health. Their emissions are monitored by national emission inventories that are the basis for emission related policies. Because of their large impact on policies these emission data should ideally be verified against independent data, such as emission estimates derived from atmospheric observations. However, this is not yet a widely established practice. Here, we present a detailed comparison of NO$_x$ emissions from the Dutch national emission inventory with completely independent emission data derived with the DECSO algorithm from satellite observations by TROPOMI on board of sentinel 5-P. This is enabled by the introduction of a new high-resolution DECSO version DECSO-HR 6.5. We find good agreement in overall emission levels, the spatial emission pattern, the 5-year emission trend, and regional emissions, with deviations in the yearly variation of emissions and at large point sources. Our results demonstrate the robustness of the national inventory and the satellite-derived emissions. This approach might serve as a use-case for the adoption of similar methods in other countries.

30 **1 Introduction**

Nitrogen oxides (NO_x) are among the most important air pollutants. Besides their negative effect on human health, they also impact the nitrogen cycle leading to eutrophication and acidification and contribute to climate change. For these reasons, the European Union imposes strict regulations on nitrogen oxide emissions. As part of the emission monitoring, national emissions of nitrogen oxides have to be reported as part of the Convention on Long-

35 Range Transboundary Air Pollution (CLRTAP (EEA, 2024b)) and the National Emission Ceiling Directive (NECD (EEA, 2024a)) of the European Union. To assess if countries adhere to their emission targets, detailed bottom-up emission inventories are compiled by each Member State. Although this legislature has been successful in reducing European NO_x emissions, the Member States of the European Union combined still emitted 1640 kt NO_x (expressed as N) in 2022 (according to NEC reporting (EEA, 2024b)), of which the Netherlands, as a small,

40 but industrialized and densely populated Member State, are responsible for 58 kt (N) (Staats et al., 2025). Although the Netherlands are expected to hit their 2023 NEC emission reduction targets, NO_x emissions contribute significantly to the so-called nitrogen crisis in the Netherlands which centers around nitrogen deposition in protected nature areas, of which about 30% is related to NO_x emissions (Hoogerbrugge et al., 2023). Therefore, monitoring and reduction of NO_x emissions remains crucial. Since the national emission inventories are the basis

45 for policies on emissions and air quality, they are very impactful and would ideally be verified against independent data.

Besides the national inventories, there also exist global and regional emission inventories, for example the Emissions Database for Global Atmospheric Research (EDGAR, (Olivier et al., 2021)) or the emission inventories provided by the Copernicus Atmospheric Monitoring System (CAMS, (Kuenen et al., 2022; Soulie et al., 2024)).

50 However, these inventories usually rely on the same or similar methods and data as the national inventories. A truly independent method to assess emissions of air pollutants are so called *top-down* methods based on atmospheric observations. In these approaches, the concentrations of air pollutants in the atmosphere are derived from observations by ground-based stations or satellites, which are then used to infer emissions. There exist different methods to solve this inverse problem, like the divergence method (Beirle et al., 2023), plume fitting

55 (Beirle et al., 2011) and inverse modelling (Miyazaki et al., 2012; Stavrakou et al., 2008). An established inverse modelling algorithm to derive emissions using satellite observations is DECSO (Daily Emissions Constrained by Satellite Observations) (Mijling & van der A, 2012). This algorithm has been widely used for a variety of different regions and gases and has been shown to show good correlation with national inventory emissions of NO_x and NH_3 for European countries (Ding et al., 2024; van der A et al., 2024). DECSO has also been applied to study the

60 effect of COVID on NO_x emissions in China (Ding et al., 2020) and the emissions of large cities and point sources (van der A et al., 2024).

In principle, as an independent method, inverse modelling provides the ideal data for validation or verification of bottom-up emission inventories: an independent emission dataset that the inventory can be compared against. Operational national verification schemes using inverse modelling have been established for different greenhouse

65 gases for a number of countries, for example Switzerland (FOEN, 2025) and the UK (Brown et al., 2025). However, there are so far only few comparable verification activities for air pollutants such as nitrogen oxides. A pilot study over satellite-based NOx verification in Germany found good agreement between the bottom-up inventory and satellite-derived emissions (Dammers et al., 2023). Few Informative Inventory Reports on air pollutants include a comparison with satellite-derived emissions of air pollutants for verification purposes, among

70   them Germany (UBA, 2025) and the Netherlands (Staats et al., 2025). While the DECSO algorithm has been
      widely used for a variety of different regions and gases (Ding et al., 2024; van der A et al., 2024), it has not yet
      been thoroughly applied for emission verification on a national and subnational scale.

      In this paper, we therefore present a detailed comparison of the Dutch national emission inventory and emission
      data generated by DECSO with the goal to verify the national emission inventory that forms the basis for emission

75   policies. To that end, a high resolution version of DECSO-HR was developed and a new version DECSO 6.5 is
      introduced. NO_x emissions for a focus region centred on the Netherlands were derived from TROPOMI (on board
      of the satellite S5P) observations. The national inventory and DECSO-HR 6.5 showed good agreement of spatial
      emission patterns with a general agreement in total annual and monthly national emissions. On the other hand, the
      respective emission trends showed deviations in the years 2020 and 2021 and there were local deviations at

80   locations with high emission intensities. We also explore the possibilities for emission verification on provincial
      and municipal levels. This detailed comparison for the Netherlands might serve as a use-case for other countries
      and forms a starting point for a new NO_x emission verification and monitoring regime in the Netherlands.

2 Methods and data sources

2.1 DECSO

85   The inversion algorithm DECSO (Daily Emissions Constrained by Satellite Observations) has been developed at
      KNMI for the purpose of deriving emissions for short-lived gases (Mijling & van der A, 2012). DECSO is using
      a Kalman Filter implementation for assimilating emissions, which includes the following steps: The sensitivity
      matrix (or Jacobian) to describe the relation between gridded emissions and satellite observations is derived using
      an ensemble of trajectories calculations with an estimated effective lifetime of the trace gas. The satellite

90   observations are compared to the concentrations modelled by the chemical transport model (CTM) CHIMERE
      v2020r3 (Menut et al., 2021). The difference between model and observations is used to adapt the emissions
      within the data assimilation scheme. Since these adaptations are based on additions or subtractions and no scaling
      is involved, emerging or disappearing emission sources are also detected. Note that the a-priori emissions are not
      from an external inventory but based on the emissions of the previous day. DECSO is currently designed to

95   estimate NOx and/or NH_3 emissions. Detailed information on the inversion method can be found in Mijling and
      Van der A (2012).

      For deriving NOx emissions, we use NO_2 observations of the TROPOMI instrument on board Sentinel 5P (van
      Geffen et al., 2022). Only observations with a cloud radiance fraction of less than 50% (this corresponds to a
      cloud fraction of about 20%) are selected for input to DECSO, which is about 50% of all observations. The

100   precision of the derived NOx emissions is estimated as 8% for annual emissions and 25% for monthly emissions
      (van der A et al., 2024).

      The version we used at the start of this study is version 6.4. It is actually the same code as version 6.3, published
      in van der A et al. (2024), Ding et al. (2024), and Lin et al. (2024), except that the vertical emission profiles for
      industrial sources used in the CTM were updated following the analyses of Bieser et al. (2011). In this study we

105   focused on the Netherlands (50-54 North, 2-9 East), which is a relatively small country, and a higher resolution
      emission grid of NOx emissions was required for a detailed intercomparison. To facilitate such an intercomparison
      a new high-resolution version of DECSO was developed named DECSO-HR. While the original version of

DECSO had a 0.1° resolution, the newly developed DECSO-HR focussed on the Netherlands at a 0.05° resolution, comparable to the resolution of the TROPOMI observations, which are 3.5 x 5.5 km at nadir. Together with additional developments of the algorithm to improve its quality, this has led to the release of version 6.5. Some of these points of improvement were notably revealed by the comparison to the Dutch emission inventory.

The changes from 6.4 to 6.5 included some minor corrections such as including the seasonal cycle of VOCs, adapted vertical emission profiles for ship emissions and an error correction for high concentrations to avoid the assimilation to favour the majority of low emissions in the region. The main changes that will be discussed below were related to the use of a new superobservation code, a correction of NO_2 observations in winter, and a fixed lifetime specifically for the high-resolution version.

DECSO is using superobservations, which are area-weighted means of cloud-free TROPOMI observations over the model grid cells. The software to construct these superobservations has been replaced by the software of Rijsdijk et al. (2025), which provides a more realistic description of the superobservation uncertainties. At the same time, the observations of the tropospheric column till 500 hPa are calculated. However, these superobservations are not used for the HR-version of DECSO because the model grid and the TROPOMI resolution are almost equal and the advantage of superobservations disappears. For the HR version the tropospheric column of NO_2 till 500 hPa is used directly as input to DECSO. Another change for the HR-version of DECSO is that the effective lifetime of NOx is no longer derived locally but fixed to 3 hours. This significantly improves the calculation time at the cost of slightly slower convergence speed to match the emissions to the observations.

During this study we noticed the TROPOMI NO_2 observations were unrealistically low or even negative during days in the winter with strong wind coming from northerly to westerly directions. This was corrected by using a reference sector above a relatively clean area over the North Sea to determine the bias between the CTM of DECSO and the NO_2 retrievals. The effect of this correction can also be seen in Fig. 3b.

Although DECSO provides additional information on anthropogenic emission and soil emissions (Lin et al., 2024), in this paper only the total NO_x emissions are analysed.

2.2 Dutch Emission Inventory

The national Dutch emission inventory (in Dutch *Emissieregistratie*) reports emissions for 375 different substances towards air and water, including the most important air pollutants like NO_x, SO_x and particulate matter and all greenhouse gases. It also compiles the Informative Inventory Report about air pollutant emissions (Staats et al., 2025) which is annually published to fulfil obligations under CLRTAP and NECD. The methods used to calculate emissions are detailed in the yearly method reports of each sector (Honig et al., 2025; van der Zee et al., 2025; Visschedijk et al., 2025; Witt et al., 2025). Most data from the emission inventory, including spatial gridded data and emissions per province and municipality for this analysis were downloaded from https://www.emissieregistratie.nl/data. Some additional data like the large point source data were produced by the emission inventory on special request.

2.3 Data analysis

To calculate national, provincial and municipal Dutch emissions from the satellite data, grid cells within the Netherlands, excluding the Dutch part of the North Sea, were selected using the exactextractr package in R

(Baston, 2024). For grid cells partially in an area, the emissions were distributed based on the share of the grid cell within the Netherlands. Regridding of inventory data to the DECSO resolution was carried out using the resample function of the terra package in R by calculating mean fluxes (Hijmans, 2025). Monthly inventory emissions were calculated by mapping the emissions from the emission inventory to GNFR sectors in order to use temporal emission profiles from the CAMS-TEMPO v4.1 data set (Guevara et al., 2021). The majority of NOx emissions in L_AgriOther in the Netherlands is from application of manure to agricultural soils. However, the profile for NOx emissions from L_AgriOther in CAMS-TEMPO is based on burning of agricultural waste, a practice not legal in the Netherlands. Therefore, the profile for NH$_3$ was used instead.

2.4 Other data sources

For additional emission data outside the Netherlands CAMS-REG-ANT v8.1 was used (Kuenen et al., 2022). Monthly emissions were estimated using CAMS-TEMPO v4.1 (Guevara et al., 2021). Official national, provincial and municipal borders of the Netherlands were downloaded from PDOK (2024). Information on the Dutch road network were downloaded from RWS (2024).

2.5 Uncertainties

The uncertainty of the NOx emissions quantified with DECSO at the scale of the Netherlands was estimated as 8% (95% confidence interval). Additional uncertainties arise from the applied country mask, which have so far not been quantified. The uncertainty of NOx emissions in the Dutch National Inventory was calculated with a Monte-Carlo analysis based on the estimated uncertainties of individual emission sources and was found to be 19% (95% confidence interval) (Staats et al., 2025). Uncertainties in the spatial or temporal distribution of the Dutch National Inventory have so far not been analysed.

3 Results and Discussion

3.1 Inventory emissions and satellite observations show qualitative agreement

Figure 1 shows a comparison of emissions maps for the year 2019 as reported by the Dutch national emission inventory and as derived from satellite observations analysed with the DECSO algorithm (total emissions) using the original DECSO 6.4.1 at 0.1° resolution and the newly introduced DECSO-HR 6.5 with a resolution of 0.05°. As the Dutch national emission inventory covers only the Netherlands, emissions for neighbouring countries were added from CAMS-REG-ANT (Kuenen et al., 2022). To allow for an easier visual comparison, the inventory dataset is also shown interpolated to the resolution of DECSO-HR of 0.05°.

First, comparing DECSO 6.4.1 and DECSO-HR 6.5, the increased resolution clearly provides additional detail. While large emission hotspots within and outside the Netherlands, like Amsterdam, Rotterdam, Antwerp and the Rhine-Ruhr area can be recognized in both data as reported earlier (van der A et al., 2024), the improved resolution of DECSO-HR 6.5 reveals additional valuable details, like distinguishing the emissions from Amsterdam and the industrial complexes in IJmuiden (in the North-West of the Netherlands, see also Fig. 2) or resolving individual emission hotspots within the German Rhine-Ruhr area (in the South-East of the domain).

Next, the comparison between DECSO-HR 6.5 (Fig. 1b) and the national emission inventory (Fig. 1c,d) directly shows the good spatial agreement between these two independent emission datasets. Both emission maps clearly

show the urban emission hotspots of Amsterdam, Rotterdam and Utrecht in the Western part of the Netherlands. On the inventory emission maps one can also clearly recognize the network of high-ways and rivers (used for inland navigation) in the Netherlands. These features are also indicated in the DECSO-HR 6.5 emission map (Fig.

185 1b), while being completely unrecognizable in DECSO 6.4.1. Interestingly, while not all shipping routes on the North Sea in the inventory dataset are resolved in DECSO-HR 6.5, the main shipping routes towards Rotterdam and Antwerp are still captured.
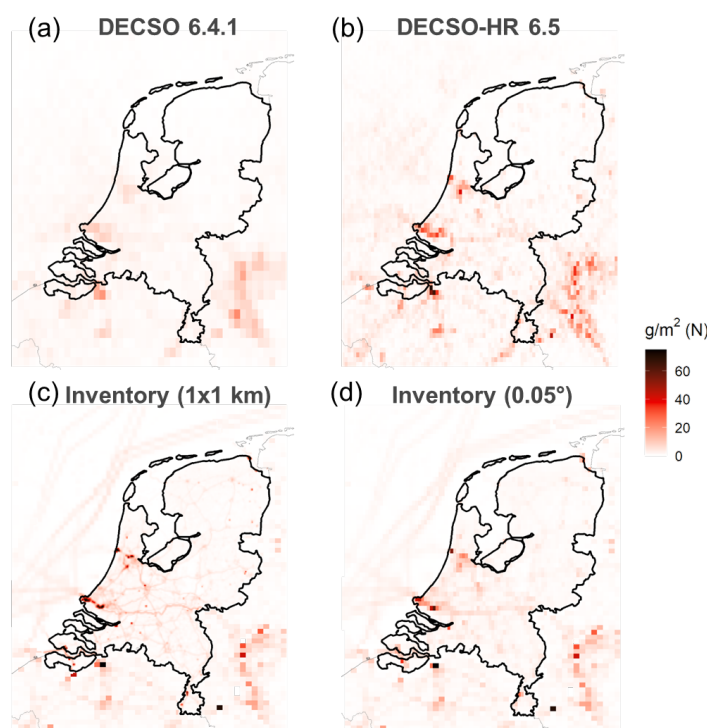
Figure 1: Maps of annual NOₓ emissions for 2019 according to satellite observations analysed with (a)
190 **DECSO 6.4.1 (0.1° resolution), (b) DECSO-HR (0.05° resolution), (c) the Dutch national emission inventory on 1 km resolution and (d) interpolated to 0.05°. Inventory emissions outside the Netherlands are added from CAMS-REG-ANT (at a resolution of 0.05°x0.1°). To allow better visualization fluxes in (c) were limited to 75 g/m².**

Zooming closer on the biggest cities Rotterdam and Den Haag (Fig. 2, left) and Amsterdam (right) and their
195 surrounding industrial areas in DECSO-HR 6.5, one can clearly see the good correlation between registered point sources (blue circles) and the satellite emissions estimates. Also Schiphol airport (runways marked with purple diamonds) is clearly visible in the satellite data set. Interestingly, the highway network around these cities (indicated in rainbow colors) is not visible in the DECSO-HR emission maps despite road traffic being a major source of NOₓ as will be discussed in more detail below.
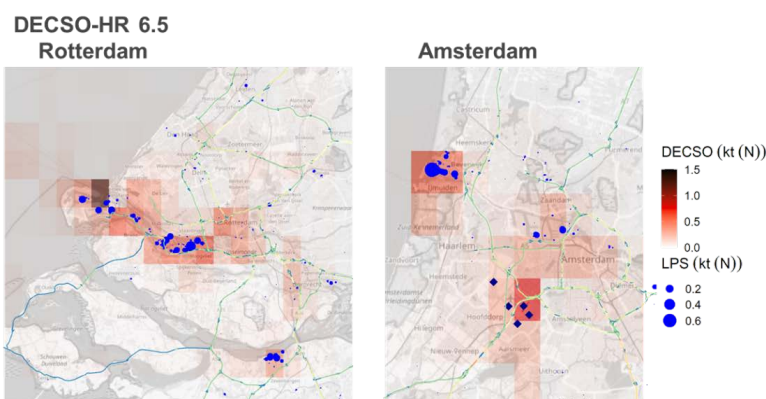
Figure 2: Zoom-ins on the urban and industrial areas in and around Rotterdam and Amsterdam. Blue circles mark point sources, highways are shown as lines with the colour indicating the number of lanes (increasing from blue to red), purple diamonds mark the runways of Schiphol airport. Map data © OpenStreetMap contributors 2025. Distributed under the Open Data Commons Open Database License (ODbL) v1.0.

3.2 Comparison of annual and monthly national total emissions

Next, for a quantitative comparison of the emission inventory with satellite-based emission estimates, we compare the timeseries of total national emissions from 2019 to 2023 for DECSO 6.4.1 and DECSO-HR 6.5 as shown in Fig. 3. To calculate national total emissions from the DECSO datasets, grid cells within the Netherlands, excluding the Dutch part of the North Sea, were added up. For the time span investigated here, the national inventory reported monotonously decreasing emissions from 76 kt (N) in 2019 to 61 kt (N) in 2023 (Staats et al., 2025). In comparison, DECSO 6.4.1, the latest version of DECSO when this work started, reported only 44 kt (N) in 2019. By contrast, DECSO-HR 6.5 was much closer to the inventory with 68 kt (N) in 2019 and agrees with the inventory within the uncertainty range for all years except for 2021.

There is, however, a notably difference in the inter-annual variation between the different emission data: While the inventory emissions decline monotonously from 2019 to 2023, DECSO-HR 6.5 reports a minimum in 2021 and an increase from 2021 to 2022. This might be due to the effects of the COVID pandemic not being captured accurately by the emission inventory. While changes in the activity data, i.e. the economic activity, were presumably accurately captured by national statistics, there are also possible, less obvious effects on the emission factors, for example lower emission factors from road traffic as traffic was less congested. While there were attempts to also include these effects, these certainly lead to higher uncertainties in the inventory emissions that are so far not well understood. These data thus might imply that emission reduction during the pandemic was underestimated by the national inventory, but other explanations are also feasible, for example meteorological conditions.

Despite these differences, fitting a trendline to the emissions from both DECSO-HR 6.5 and the inventory (dashed line in Fig. 3a) led to similar emission trends with a yearly reduction of 3.1 kt (N) for DECSO-HR6.5 and 3.3 kt (N) for the inventory, showing that emission trends on intermediate timescales of several years agree between the two data sets.

Besides the inter-annual emission trend, we also compared the intra-annual variation of emissions. Therefore, mean monthly emissions from satellite observations were compared to monthly inventory emissions (Fig. 3b). As the Dutch national inventory only produces annual emissions, monthly inventory emissions were estimated by

distributing the inventory emissions per GNFR sector using the CAMS-TEMPO temporal profiles (Guevara et al., 2021). This comparison revealed large differences in the temporal profiles. While the inventory emissions were roughly constant throughout the year with higher emissions from stationary combustion and road transport in winter being compensated by higher emissions from agriculture and non-road mobile machinery in summer,

235   DECSO 6.4.1 shows a strong minimum of emissions in winter, with emissions in January being just 20% of emissions in June (Fig. 3b). This deviation in winter also explains the large deviation in yearly emissions between the inventory and DECSO 6.4.1 in Fig. 3a. The low DECSO emissions in winter were caused by a bias in the TROPOMI NO_2 retrievals for observations with a strong north-western wind in the winter when NO_2 observations were close to zero or even negative. Correction of this bias in DECSO-HR 6.5 (see section 2.1) therefore remedied

240   this winterly mismatch. Consequently, monthly emissions according to DECSO-HR 6.5 agree within the uncertainty range with inventory emissions.

Taken together, the improvements introduced with DECSO-HR 6.5 not only provided more spatial information but also improved the match to inventory emissions.

245
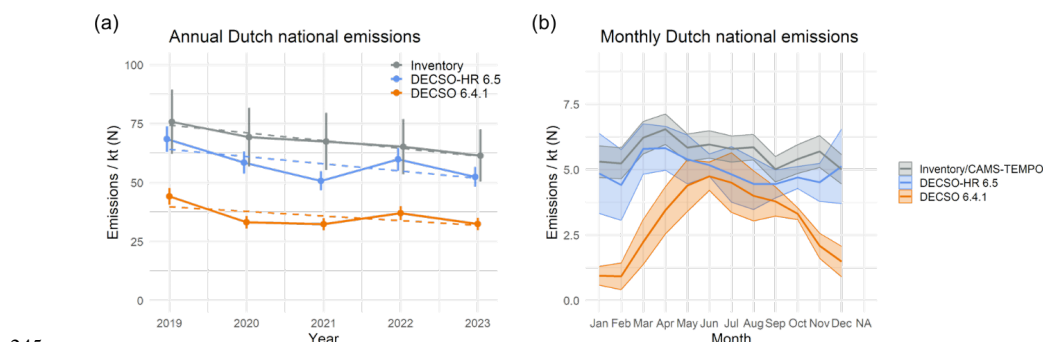
Figure 3: (a) Total annual Dutch emissions from 2019 to 2023 with trend lines shown as dashed lines and (b) Mean monthly emissions (averaged from 2019 to 2023) according to the Dutch national emission inventory (combined with CAMS-TEMPO), DECSO 6.4.1 and DECSO-HR 6.5. Error bars and the shaded area both show the 95% confidence interval.

250   **3.3 Quantitative comparison of spatially explicit emissions**

After analysing the temporal match of the emission datasets, we next considered their spatial correlation as shown in Fig. 4. Figure 4a shows a difference map for 2019 between the national inventory and DECSO-HR 6.5. In general, this map confirms the good agreement between the two data sets. There are no systematic deviations or biases apparent on a national scale and deviations could only be observed in the Amsterdam/IJmuiden and

255   Rotterdam areas (Fig. 4b). In these areas, DECSO yields overall lower emissions than reported in the inventory. Interestingly, it appears that in these areas there might be an alternating pattern of positive and negative deviations, which will be further discussed below.

In the zoom-in views of urban areas, also highways and Schiphol airport are indicated as the transport sector is the main source of NO_x emissions in the Netherlands. Schiphol airport (with purple diamond's indicating the

260   runways) is clearly visible in the DECSO emission maps (Fig. 2). Considering also the difference maps (Fig. 4b), DECSO-HR 6.5 reports higher emissions than the national inventory over Schiphol airport. This might be caused by the national inventory only reporting emissions for the landing and take-off phase of the flights (LTO) up to

3000 ft (~914 m) according to international agreements, thereby missing emissions above 3000 ft, which have been estimated at 4 kt (N) over the entire Netherlands (Witt et al., 2024) of which about 2/3 are related to air

265 traffic at Amsterdam Schiphol airport. These emissions will in parts still contribute to satellite observations of column densities. The highway network on the other hand was not very apparent in the emission maps (Fig. 2) or the difference maps (Fig. 4b), indicating that as a diffuse source road traffic will be difficult to spatially isolate in the DECSO emissions.

270
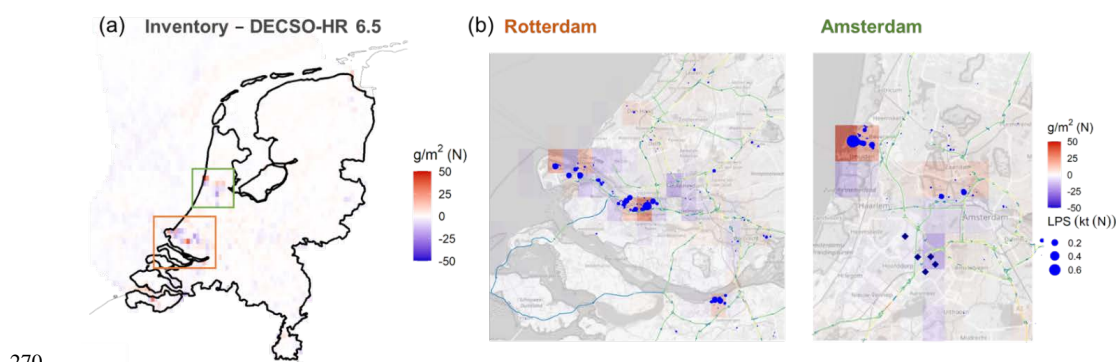
Figure 4: (a) Difference between the annual NOx emissions according the inventory and DECSO-HR 6.5 per grid cell for 2019. Red colors indicate that the inventory has larger emissions, blue that DECSO results are higher. (b) Zoom-ins on the industrial areas in and around Amsterdam and Rotterdam. Blue circles mark point sources, highways are shown as lines with the color indicating the number of lanes (increasing

275 **from blue to red), purple diamonds mark the runways of Schiphol airport. Map data © OpenStreetMap contributors 2025. Distributed under the Open Data Commons Open Database License (ODbL) v1.0.**

As these two areas around Rotterdam and Amsterdam have large industrial sides and harbours and consequently high emissions, we hypothesized that the deviation between the two datasets was depending on the intensity of

280 the fluxes. To further explore these deviations, emissions according to DECSO-HR 6.5 were plotted per grid cell as a function of the inventory emissions in that same grid cell (Fig. 5a), which revealed two different behaviours at low and high emissions. At low emissions (below roughly 0.25 kt (N), yellow shading) emissions per grid cells showed on average good correlation (dark blue circles), albeit with some scatter. At larger emissions (blue shading), however, the two datasets started to deviate, with the mean DECSO emissions moving further and

285 further from the unity line. This can be seen even more clearly when considering the difference between the two datasets as a function of inventory emissions (Fig. 5b). The mean deviation was close to 0 at small emissions below 0.25 kt (N) (yellow shading) and started to increase at higher emissions (blue shading). It reached 0.5 kt (N) for grid cells with emissions around 1 kt (N), a deviation of almost 50% for these highly-emitting grid cells. These deviations at high emissions had a large impact on the total estimated national emissions: Grid cells with

290 an emission larger than 0.5 kt (N) in the emission inventory were responsible for 53% of the observed deviation between inventory and satellite observations on a national scale in 2019, despite representing only 0.4% of grid cells.

This leads to the question where these large deviations are coming from, an underestimation by the satellite-derived emissions or an overestimation by the inventory. On the inventory side, these high-emission grid cells

295 relate to areas of high industrial activity whose emissions are registered as large point sources. The quantity of

these emissions is being reported by the companies themselves, according to standardized methods and controlled by local environmental authorities (Staats et al., 2025). That means that the location of these emission sources is precisely known leading to neglectable spatial uncertainty. On the other hand, while there are certainly uncertainties in the amount of emissions, there are no records of systematic overreporting of industrial emissions.

300 Looking at satellite-derived emissions, a part of this deviation might be explained by the emissions from large point sources being wrongly allocated to neighbouring grid cells, in other words appearing smeared out over a larger area. This would lead to an alternating pattern of over- and underestimated grid cells, as can indeed be seen in Fig. 4b. However, while this fits qualitatively, these alternating pixels do not compensate each other quantitively, meaning that even when adding these grid cells up DECSO reports lower emissions for highly

305 emitting areas than the inventory. In absence of a known ground truth, more research and further independent assessments will be needed to fully understand these deviations.

Figure 5c shows the same data as fig. 5a but plotted on a double-logarithmic scale in order to better assess grid cells with low emissions, which are dominated by diffuse sources. Here, again, different behaviours can be distinguished. At very low inventory emissions below 0.01 kt (N), the DECSO emissions reached a plateau at

310 around 0.01 kt (N), which is presumably caused by NOx emissions from soils. The overall contribution of these grid cells to the total emissions is very small with only 3%, despite representing 22% of all grid cells. Above 0.01 kt (N) the two data show a good correlation, however with a slight offset towards inventory emissions. This means that also in these low-emitting grid cells the inventory reports on average higher emissions than DECSO, albeit with a very small difference.

315 Taken together, a good spatial correlation between the two emission data sets was observed, with deviations at both ends of the emission range. Of these two deviations, however, the one at low emissions hat a negligible impact on overall emission levels, while the deviation at high emissions had a major impact.
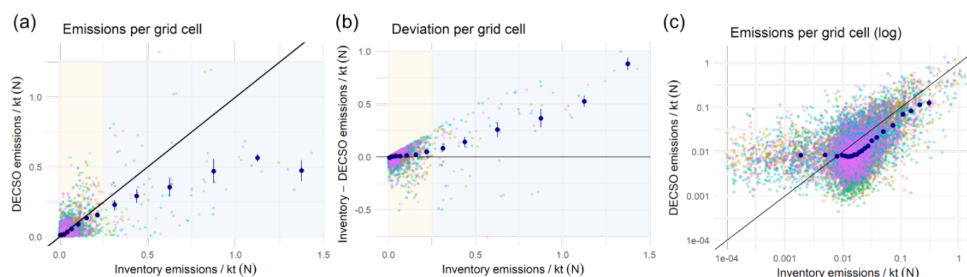
Figure 5: (a) Correlation between the two emission datasets per grid cell. The unity line is shown in black. (b)
320 **Difference between the two emission estimates per grid cell as a function of the emission of that grid cell according to the Dutch national emission inventory. (c) Same as (a) but on a log-log scale. Dark blue dots are the average of all grid cells over all years, error bars show standard errors, yellow and blue shadings mark the low and high emission behaviour, respectively.**

3.4 Possibilities for emission verification from regional to municipal scale

325 The high resolution of the DECSO-HR algorithm of 0.05° (about 5 km in the Netherlands) becomes comparable to the size of cities, municipalities and provinces, which might allow comparison and verification of inventory emissions even on these smaller scales. This could be potentially very useful, not only for a better understanding of emission sources, but also because emissions at the local scales have a high relevance for policies.

Here, we will evaluate these possibilities for the use-case of the Netherlands beginning on the scale of provinces
330 (Fig. 6a), of which there exist 12 in the Netherlands, with populations ranging from 390 000 to 3 800 000 and
land areas between 1400 and 5400 km². Comparing the emissions per province according to the inventory and
according to DECSO-HR 6.5, we see good agreement between the two data sets. A linear fit revealed a slope of
0.89 with R^2 of 0.93. That means that a small bias remains, where also on a provincial level the emission inventory
reports slightly higher emissions than DECSO-HR 6.5. However, the good correlation supports the possibilities
335 of emission verification by satellite observations also on the regional scale.

Next, we zoom-in closer, looking at the scale of municipalities (in Dutch *gemeenten*), which can have a size as
large as 523 km² and as small as 7 km² with a population of up to 930 000 for the bigger cities but also as small
as 1000 (Fig. 6b, c). This analysis reveals even on this finer scale a good correlation, which can visually be better
appreciated on a log-log scale (Fig. 6c). Fitting a trendline returned a slope of 0.67 with R^2 of 0.84. While most
340 of the data points in general follow the unity line with some added scatter, systematic deviations can be observed
especially for municipalities with very large emissions, most prominently Rotterdam, Amsterdam, Velsen and
Vlissingen. This can be explained by the deviation between DECSO-HR 6.5 and the inventory at high emissions
discussed above (Fig. 5), which subsequently leads to a deviation for municipalities with strong industrial sources.
Furthermore, emissions in grid cells that are divided between two municipalities are split between these two
345 municipalities based on area, which effectively spreads out the emissions and leads to an underestimation of highly
emitting municipalities. To test the impact of the improved resolution on this analysis, it was repeated after
aggregating the DECSO data to a cell size of 0.1°. This led to a much worse correlation between the two datasets
with a slope of 0.566 and R^2 of 0.75. Taken together, these analyses showed that while the higher resolution did
improve the agreement between inventory and DECSO data on a municipal scale, there are still some
350 discrepancies on these spatial scales.
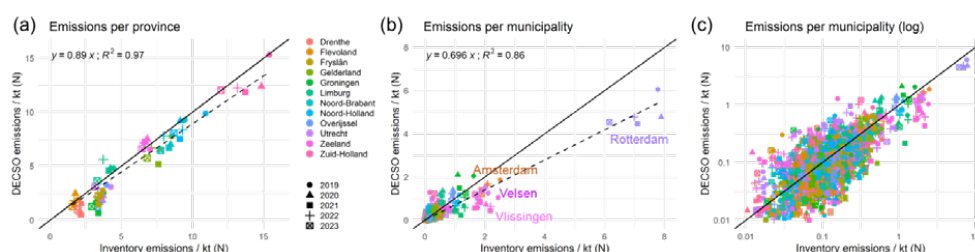
**Figure 6: (a) Comparison of annual NOx emissions according to DECSO-HR 6.5 and the Dutch national emission
inventory (a) per province, (b) per municipality on a linear scale, and (c) per municipality on a double-logarithmic
355 scale. Unity is shown as a solid line, while the dashed line represents a linear fit.**

4 Conclusion

In this paper the detailed comparison of two completely independent emission datasets - from a national emission
inventory and based on satellite observations – was presented for the use-case of the Netherlands. This comparison
was facilitated by the development of DECSO-HR 6.5, a new high-resolution version of DECSO that achieves a
360 resolution of 0.05°. It was found that the Dutch national inventory and DECSO-HR 6.5 agreed with respect to
general emission levels, the 5-year emission trend and their spatial and seasonal patterns. This good agreement
lends credibility to both of them, thereby hopefully also nurturing public trust in emission data. On the other hand,

we found that both data sets deviated for large point sources and grid cells with high emission intensities. Also both datasets showed differences in their inter-annual variability.

365 While there are some indications for the reasons behind these differences, they could not be fully explained yet. However, these observations will nevertheless be useful in guiding future research and development of both the national inventory as well as the analysis of satellite observations. For example, the comparison between the two emission data sets already aided in the correction of the winter emissions in the development of DECSO 6.5 (shown in Fig. 3b) by directing development effort towards this phenomenon.

370 In the long term, these developments will help the two methods to converge and to close the gap between these two independent ways to assess emissions. This will not only further increase their credibility, but it also means that they can be used together to support each other with their individual strengths and weaknesses. If satellite observations and emission inventories are consistent with each other, one can fully utilize the quick turnover of satellite observations that can deliver emissions in almost real time, instead of the 2 year lag of inventories.

375 Conversely, the inventories can provide sector information and spatial details that are not attainable by satellite observations. In this way, these two methods can synergies with each other to build a stronger and faster emission monitoring regime.

Data Availability

380 Data from the Dutch national inventory is available from https://www.emissieregistratie.nl/data. Data from the DECSO algorithm is available from https://www.temis.nl/emissions/decso_nox.php. The data and scripts used to generate the figures in the manuscript will be made available on a repository upon publication.

Author Contribution

385 HW, RJvdA and MCvZ conceptualized the research. RJvdA and JD developed the DECSO algorithm and provided input on the interpretation of DECSO emissions. HW, JK and MCvZ provided input on the interpretation of inventory emissions. HW processed the data for the comparison, which was discussed between all authors. HW wrote the manuscript with input from all authors.

390 **Funding**

This work has been funded by the DECSO-NRT-Europe project of the Sentinel Users Preparation initiative of ESA to KNMI, the European Union's Horizon research and innovation programme under grant agreement No. 101183071 (GreenEO) to KNMI and No. 101081322 (AVENGERS) to RIVM, and the Ministry of Climate Policy and Green Growth (Ministerie van Klimaat en Groene Groei, *Versterkingsgelden Klimaat*) to RIVM.

395

Competing interests

The authors declare that they have no conflict of interest.

Acknowledgement

400 We thank Marc Guevara Vilardell for providing the CAMS-TEMPO data and support in interpreting the temporal profiles and Henk de With for generating the point source dataset.

5 References

Baston, D., exactextractr: Fast Extraction from Raster Datasets using Polygons:
  https://isciences.gitlab.io/exactextractr/, last access: 01.12.2025.

Beirle, S., Borger, C., Jost, A., and Wagner, T.: Improved catalog of NOx point source emissions (version 2),
  Earth Syst Sci Data, 15, 3051–3073, 10.5194/essd-15-3051-2023, 2023.

Beirle, S., Boersma, K. F., Platt, U., Lawrence, M. G., and Wagner, T.: Megacity emissions and lifetimes of
  nitrogen oxides probed from space, Science, 333, 1737–1739, 10.1126/science.1207824, 2011.

Bieser, J., Aulinger, A., Matthias, V., Quante, M., and Denier van der Gon, H. A.: Vertical emission profiles for
  Europe based on plume rise calculations, Environ Pollut, 159, 2935–2946,
  10.1016/j.envpol.2011.04.030, 2011.

Brown, P., Cardenas, L., Vento, S. D., Karagianni, E., MacCarthy, J., Mullen, P., Gorji, S., Richmond, B.,
  Thistlethwaite, G., Thomson, A., Wakeling, D., and Willis, D.: UK Greenhouse Gas Inventory, 1990 to
  2023, Ricardo, 2025.

Dammers, E., Tokaya, J., Timmermans, R., Schaap, M., and Coenen, P.: Satellite-based Emission Verification,
  Umweltbundesamt1862-4804, 2023.

Ding, J., van der A, R. J., Eskes, H. J., Mijling, B., Stavrakou, T., van Geffen, J. H. G. M., and Veefkind, J. P.:
  NOx Emissions Reduction and Rebound in China Due to the COVID-19 Crisis, Geophysical Research
  Letters, 47, 10.1029/2020gl089912, 2020.

Ding, J., van der A, R., Eskes, H., Dammers, E., Shephard, M., Wichink Kruit, R., Guevara, M., and Tarrason, L.:
  Ammonia emission estimates using CrIS satellite observations over Europe, Atmospheric Chemistry and
  Physics, 24, 10583–10599, 10.5194/acp-24-10583-2024, 2024.

EEA: Air pollution in Europe: 2024 reporting status under the National Emission reduction Commitments
  Directive, European Environment Agency, 10.2800/019282, 2024a.

EEA: European Union emission inventory report 1990-2022 — Under the UNECE Convention on Long-range
  Transboundary Air Pollution (Air Convention), European Environment Agency, 10.2800/2893, 2024b.

FOEN: Switzerland's Greenhouse Gas Inventory 1990–2023: National Inventory Document and reporting tables
  (CRT). Federal Office for the Environment, 2025.

Guevara, M., Jorba, O., Tena, C., Denier van der Gon, H., Kuenen, J., Elguindi, N., Darras, S., Granier, C., and
  Pérez García-Pando, C.: Copernicus Atmosphere Monitoring Service TEMPOral profiles (CAMS-
  TEMPO): global and European emission temporal profile maps for atmospheric chemistry modelling,
  Earth Syst Sci Data, 13, 367–404, 10.5194/essd-13-367-2021, 2021.

Hijmans, R.J., terra: Spatial Data Analysis: https://github.com/rspatial/terra, last access: 01.12.2025.

Honig, E., Montfoort, J. A., Dröge, R., van Mil, S. E. H., Guis, B., Baas, K., van Huet, B., and van Hunnik, O. R.:
  Methodology for the calculation of emissions to air from the sectors Energy, Industry and Waste, RIVM,
  10.21945/RIVM-2025-0002, 2025.

Hoogerbrugge, R., Braam, M., Siteur, K., Jacobs, C., Hazelhorst, S., Stefess, G., Swaluw, E. v. d., Kruit, R. W.,
  Wesseling, J., and Pul, A. v.: Uncertainty in the determined nitrogen deposition in the Netherlands Status
  report 2023, RIVM, 10.21945/RIVM-2022-0085, 2023.

Kuenen, J., Dellaert, S., Visschedijk, A., Jalkanen, J. P., Super, I., and van der Gon, H. D.: CAMS-REG-v4: a state-of-the-art high-resolution European emission inventory for air quality modelling, Earth Syst Sci Data, 14, 491–515, 10.5194/essd-14-491-2022, 2022.

Lin, X., van der A, R., de Laat, J., Huijnen, V., Mijling, B., Ding, J., Eskes, H., Douros, J., Liu, M., Zhang, X.,
445   and Liu, Z.: European Soil NOx Emissions Derived From Satellite NO2 Observations, Journal of Geophysical Research: Atmospheres, 129, 10.1029/2024jd041492, 2024.

Menut, L., Bessagnet, B., Briant, R., Cholakian, A., Couvidat, F., Mailler, S., Pennel, R., Siour, G., Tuccella, P., Turquety, S., and Valari, M.: The CHIMERE v2020r1 online chemistry-transport model, Geoscientific Model Development, 14, 6781–6811, 10.5194/gmd-14-6781-2021, 2021.

450   Mijling, B. and van der A, R. J.: Using daily satellite observations to estimate emissions of short-lived air pollutants on a mesoscopic scale, Journal of Geophysical Research: Atmospheres, 117, 10.1029/2012jd017817, 2012.

Miyazaki, K., Eskes, H. J., and Sudo, K.: Global NOx emission estimates derived from an assimilation of OMI tropospheric NO2 columns, Atmospheric Chemistry and Physics, 12, 2263–2288, 10.5194/acp-12-2263-
455   2012, 2012.

Olivier, J., Guizzardi, D., Schaaf, E., Solazzo, E., Crippa, M., Vignati, E., Banja, M., Muntean, M., Grassi, G., Monforti-Ferrario, F., and Rossi, S.: GHG emissions of all world – 2021 report, Publications Office of the European Union, doi/10.2760/173513, 2021.

PDOK, Dataset: Bestuurlijke Gebieden: https://www.pdok.nl/introductie/-/article/bestuurlijke-gebieden, last
460   access: 01.05.2024.

Rijsdijk, P., Eskes, H., Dingemans, A., Boersma, K. F., Sekiya, T., Miyazaki, K., and Houweling, S.: Quantifying uncertainties in satellite NO2 superobservations for data assimilation and model evaluation, Geoscientific Model Development, 18, 483–509, 10.5194/gmd-18-483-2025, 2025.

RWS,   Weggegevens - maximumsnelheden en rijbanen (WEGGEG): https://inspire-
465   geoportal.ec.europa.eu/srv/api/records/abaf1e22-55aa-4a11-a855-7ac963e4a82b,   last   access: 29.05.2024.

Soulie, A., Granier, C., Darras, S., Zilbermann, N., Doumbia, T., Guevara, M., Jalkanen, J.-P., Keita, S., Liousse, C., Crippa, M., Guizzardi, D., Hoesly, R., and Smith, S. J.: Global anthropogenic emissions (CAMS-GLOB-ANT) for the Copernicus Atmosphere Monitoring Service simulations of air quality forecasts and
470   reanalyses, Earth Syst Sci Data, 16, 2261–2279, 10.5194/essd-16-2261-2024, 2024.

Staats, N., Bolech, M., Dellaert, S. N. C., Dröge, R., van Eijk, E., Honig, E., van Huet , B., van Huijstee, J., van Mil, S. E. H., te Molder, R. A. B., Plomp, A. J., Wever, D., Witt, H., van Zanten, M. C., and van der Zee, T.: Informative Inventory Report 2025 Emissions of transboundary air pollutants in the Netherlands 1990–2023, RIVM, 10.21945/RIVM-2025-0007, 2025.

475   Stavrakou, T., Müller, J. F., Boersma, K. F., De Smedt, I., and van der A, R. J.: Assessing the distribution and growth rates of NOx emission sources by inverting a 10-year record of NO2 satellite columns, Geophysical Research Letters, 35, 10.1029/2008gl033521, 2008.

UBA: German Informative Inventory Report 2025 (IIR 2025), Umweltbundesamt, 2025.

van der A, R. J., Ding, J., and Eskes, H.: Monitoring European anthropogenic NOx emissions from space,
480   Atmospheric Chemistry and Physics, 24, 7523–7534, 10.5194/acp-24-7523-2024, 2024.

van der Zee, T. C., Bleeker, A., van Bruggen, C., Bussink, W., van Dooren, H. J. C., Groenestein, C. M., Huijsmans, J. F. M., Kros, H., van der Most, M., Oltmer, K., Ros, M., Schulte-Uebbing, L., and Velthof, G. L.: Methodology for the calculation of emissions from agriculture, RIVM, 10.21945/RIVM-2025-0003, 2025.

485 van Geffen, J., Eskes, H., Compernolle, S., Pinardi, G., Verhoelst, T., Lambert, J.-C., Sneep, M., ter Linden, M., Ludewig, A., Boersma, K. F., and Veefkind, J. P.: Sentinel-5P TROPOMI NO2 retrieval: impact of version v2.2 improvements and comparisons with OMI and ground-based data, Atmospheric Measurement Techniques, 15, 2037–2060, 10.5194/amt-15-2037-2022, 2022.

Visschedijk, A., Meesters, J. A. J., Nijkamp, M. M., Koch, W. W. R., Jansen, B. I., and Dröge, R.: Methodology
490 for the calculation of emissions from product usage by consumers, construction and services, RIVM, 10.21945/RIVM-2025-0004, 2025.

Witt, H., Molder, R. t., and Zanten, M. C. v.: Luchtvaartemissies boven Nederlands grondgebied boven 3.000 voet, RIVM, 10.21945/RIVM-KN-2024-0012, 2024.

Witt, H., Geilenkirchen, G., Bolech, M., Dellaert, S., van Eijk, E., Geertjes, K., and Kosterman, M.: Methodology
495 for the calculation of emissions from the transport sector, RIVM, 10.21945/RIVM-2025-0006, 2025.